



RPC Detector and Analysis of Cosmic Ray

Tai-Yen Huang, Ting-Kai Hsu^a

Department of Physics, National Taiwan University, Taipei, Taiwan
Institute of Physics, Academia Sinica, Taipei, Taiwan



^aMany thanks to Chia-Yu Hsieh and Wen-Chen Chang for their guidance.

Introduction

Our research focuses on detecting high-energy cosmic rays and developing a DAQ system to assess the efficiency of an RPC gaseous ionization detector. We measure the detector's efficiency at various voltages, and observe that cosmic ray incidence over time follows a Poisson distribution, as predicted by theory.

0.1 Cosmic Ray

High-energy particles from outer space collide with atomic nuclei in the upper atmosphere, initiating a chain of decay processes. These high-energy particles are known as *cosmic rays*. Among the secondary particles produced, muons would reach the ground, where they are detected by our system.

We review a simplified muon model in quantum field theory to predict the distribution¹. The model employs a scalar field $\phi(x)$ for muons and a semi-classical scalar source $\rho(x)$, and we assume no other interactions with muons. The Lagrangian is

$$\mathcal{L} = \frac{1}{2} (\partial\phi(x))^2 - \frac{1}{2} m^2 \phi(x)^2 - g\rho(x)\phi(x) \quad (1)$$

The probability of finding n particles produced by the source is

$$P(n) = |\langle n|S|0\rangle|^2 \quad (2)$$

Where $S = T \left\{ \exp(i \int d^4x g\rho(x)\phi(x)) \right\}$ is the operator whose matrix elements are so-called *S-matrix*. We apply Taylor expansion to the S operator, and only $n, n+2, n+4, \dots$ terms contribute to the probability.

$$P(n) = \frac{1}{n!} \lambda^n \cdot 1 + \frac{1}{n!} \frac{\lambda^n}{1!} \cdot (-\lambda) + \dots = \frac{\lambda^n}{n!} \exp(-\lambda) \quad (3)$$

where $\lambda = \int d^3p/(2\pi)^3 \cdot 1/E_p |g\rho(p)|^2$. This is exactly a *Poisson distribution*.

0.2 RPC Detector

0.2.1 Ionization Detector

The structure of a gaseous ionization detector²:

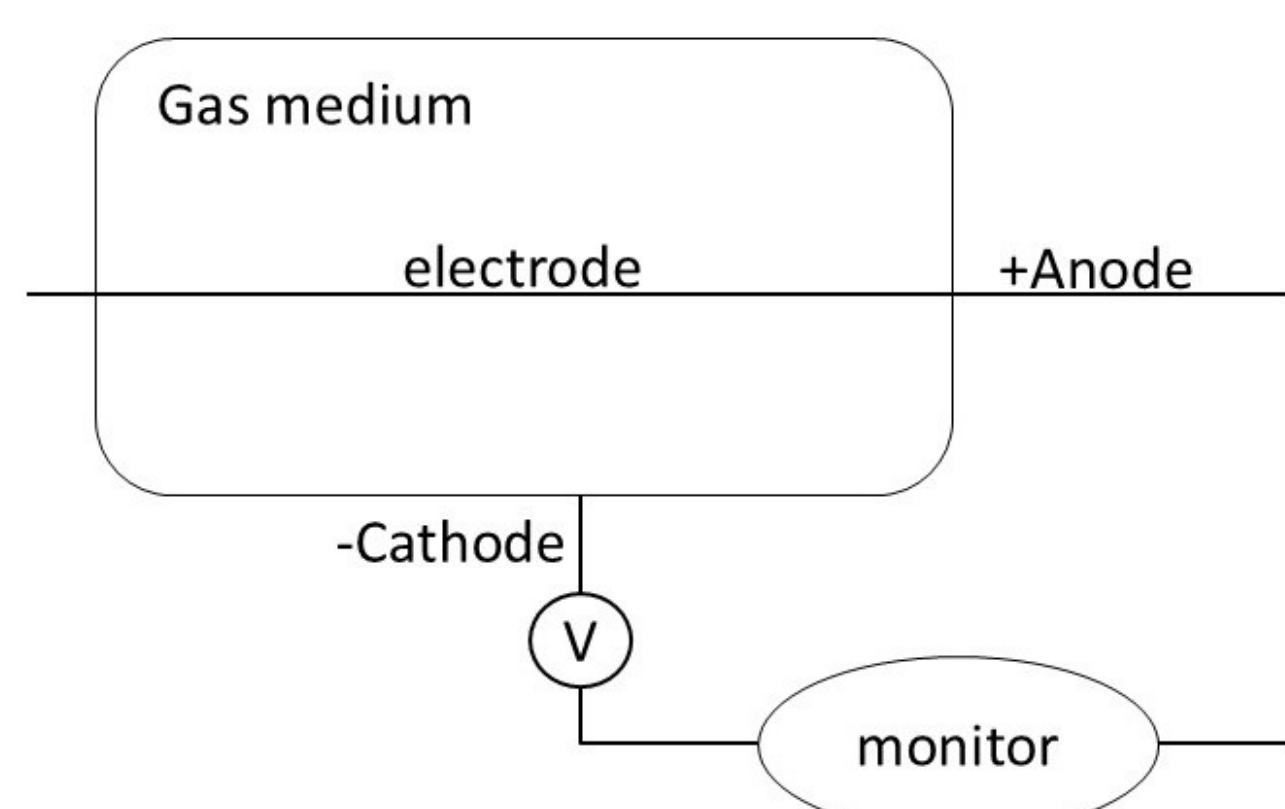


Figure 1: Structure of gaseous ionization detector.

The container is filled with a noble gas that can only be ionized by high-energy particles or ions-electrons into positive ions and free electrons. The applied voltage causes these charged particles to move toward the center and surface of the cylinder, generating a current that we can observe.

0.2.2 Resistive Plate Chambers(RPCs)

The Resistive Plate Chamber (RPC) detects charged particles by ionizing gas within a narrow gap between two resistive plates. High-energetic particle passing through creates an electron-ion avalanche, generating a localized electrical signal. RPCs are valued for their high time resolution, efficiency, and low cost. We measure RPC efficiency using cosmic rays to determine the chamber's optimal operating voltage.

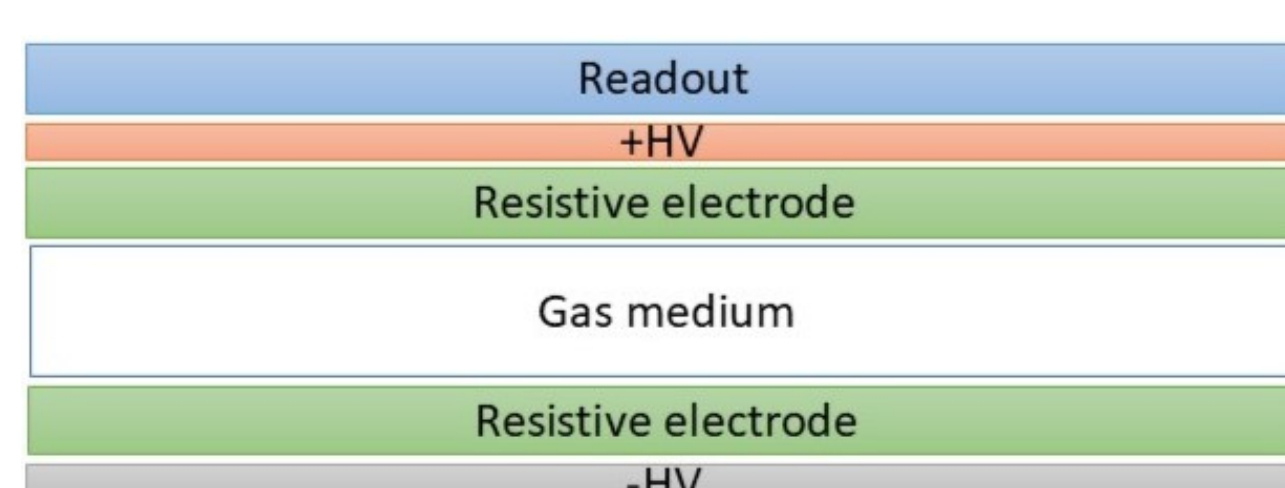


Figure 2: Structure of RPC

0.3 Trigger

Our trigger system consists of a scintillator connected to a photomultiplier.

A scintillator is a material that emits light when it absorbs ionizing radiation, such as gamma rays or charged particles. The interaction of high-energy particles with the scintillator results in the absorption of energy and re-emission as visible or ultraviolet light. This light is then detected by a photomultiplier tube (PMT). The PMT collects the light and

converts it into an electrical signal through the photoelectric effect. When the light strikes the PMT's photocathode, it generates electrons, which are accelerated and amplified by secondary dynodes, significantly boosting the electrical current. This process allows the detection and analysis of the ionizing radiation originally absorbed by the scintillator. Scintillator counters are inexpensive, fast, and easy to manufacture in large areas, making them commonly used as detectors for trigger systems.

Experimental Setting

The RPC detector is positioned between two scintillator counters that generate trigger signals for passing cosmic rays. Due to the small signal from the chamber, an amplifier is used. Measurements are taken with an oscilloscope, which visually monitors signals, and a counter that processes the digital signals from both the trigger and the RPC. Efficiency is calculated using the ratio:

$$\text{Efficiency (Eff)} = \frac{\text{Trigger AND RPC}}{\text{Trigger}} \quad (4)$$

This equation represents the ratio of events where both the trigger and RPC detect the cosmic ray to the total number of trigger events, thereby measuring the efficiency of the RPC detector.

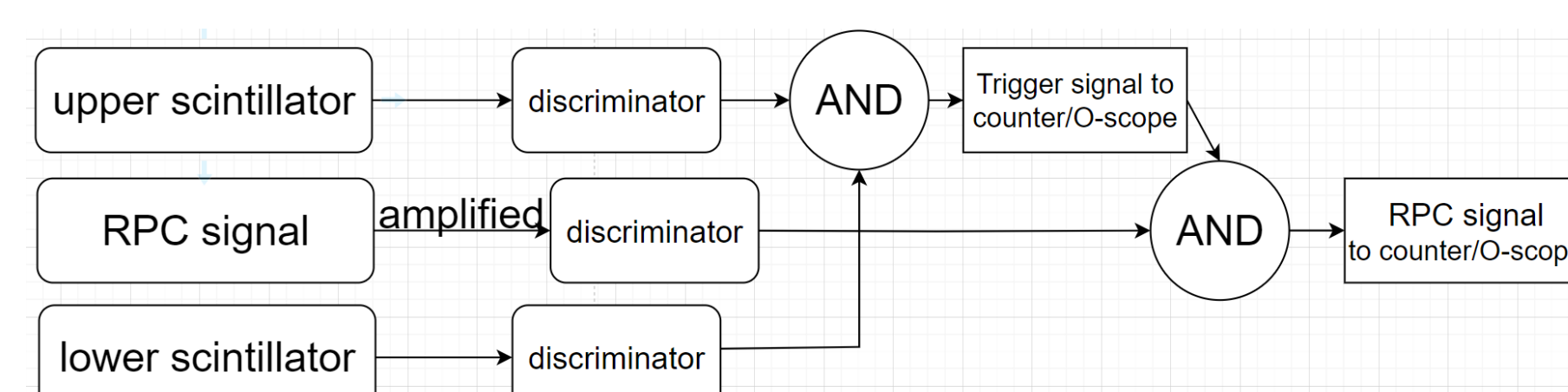


Figure 3: Setup of RPC detector and scintillator triggers

On the other hand, to understand the flux of cosmic rays at sea level, we measure the count of triggers every 20 minutes. This measurement helps determine the rate at which cosmic rays are detected, providing valuable data on the cosmic ray flux in the environment.

Distribution of Cosmic Ray and Efficiency of RPC Detector

0.4 Flux of Cosmic Ray at Sea Level

As noted in Section 0.1, the probability of detecting n muons follows a Poisson distribution.

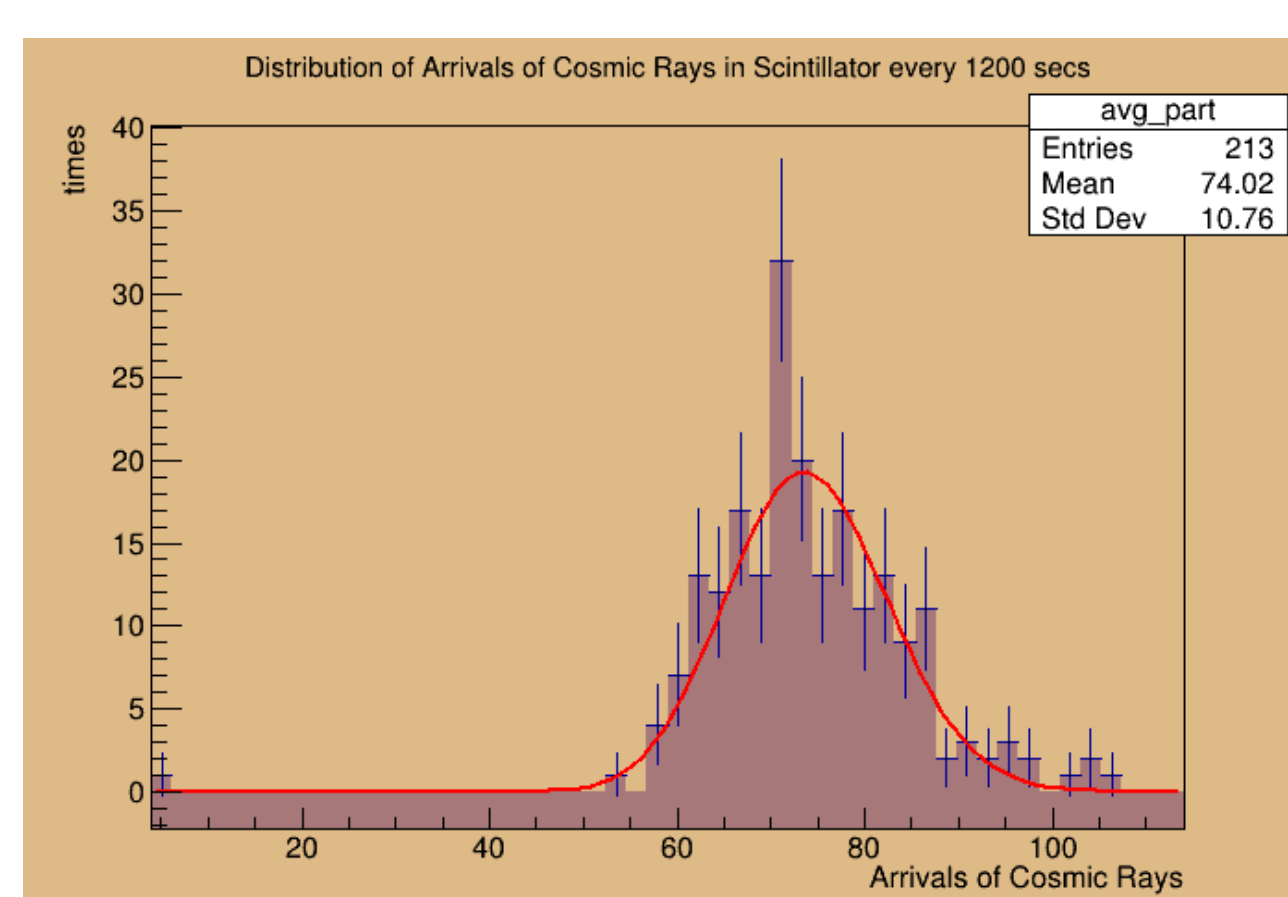


Figure 4: Arrival of Cosmic Rays in 20 mins

Poisson distribution $415.4 \text{Poisson}(x, 74.02)$ is fitted. There are 3.7 counts per minute, which is lower than the expected one³, mainly because of the efficiency and the orientation of scintillator detector.

0.5 Efficiency of RPC

Our system's efficiency is calculated as the ratio of particles detected by both the detector and the trigger to those detected by the trigger alone. When the scintillator is triggered, the oscilloscope captures data from the RPC detector to check if a particle has passed through. As shown below, there is noise in the RPC detector's waveform, which can be resolved by setting a voltage threshold.

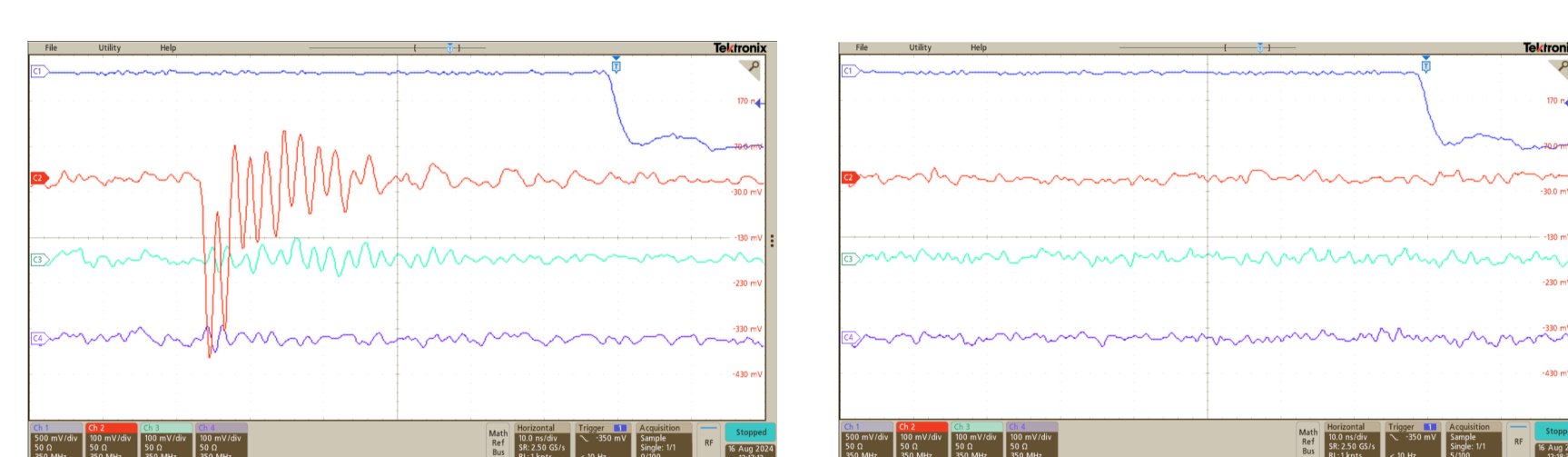


Figure 5: RPC detected particle

Figure 5: RPC didn't detect particle

0.6 Threshold determination

The distribution of noise voltage obtained from the oscilloscope is fitted with a Gaussian curve. We set the threshold at the mean minus three sigma $\mu - 3\sigma$ of the distribution of noise voltage.

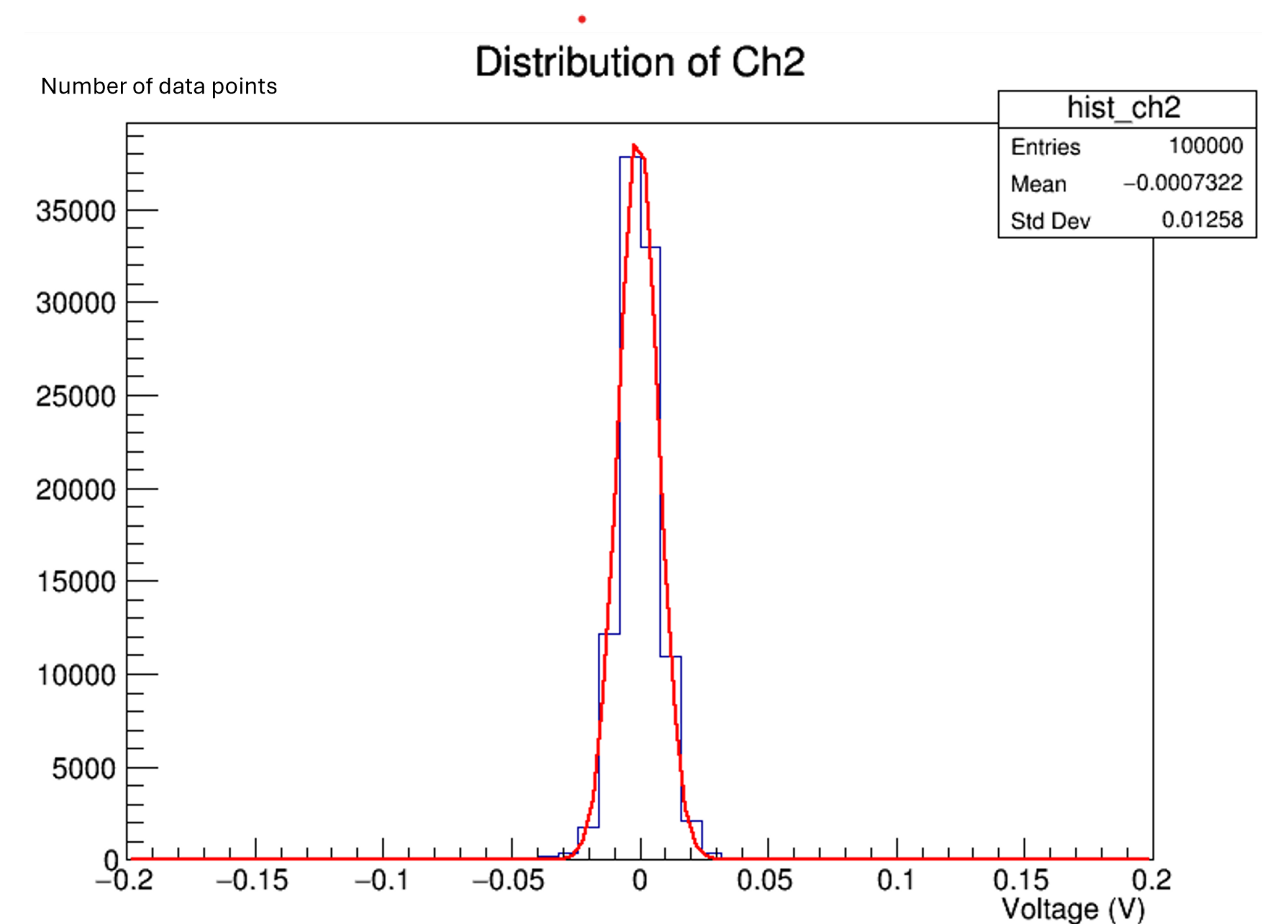


Figure 6: Fitting gaussian on noise distribution plot

	ch2	ch3	ch4	avg.
Threshold	0.029	0.021	0.024	0.025

Table1: Threshold in different voltage with Gaussian fitting method

The efficiency of the RPC detector is shown in the figure below. We observe that as the voltage increases, efficiency rises, reaching a saturation value of 0.8 at approximately 13kV.

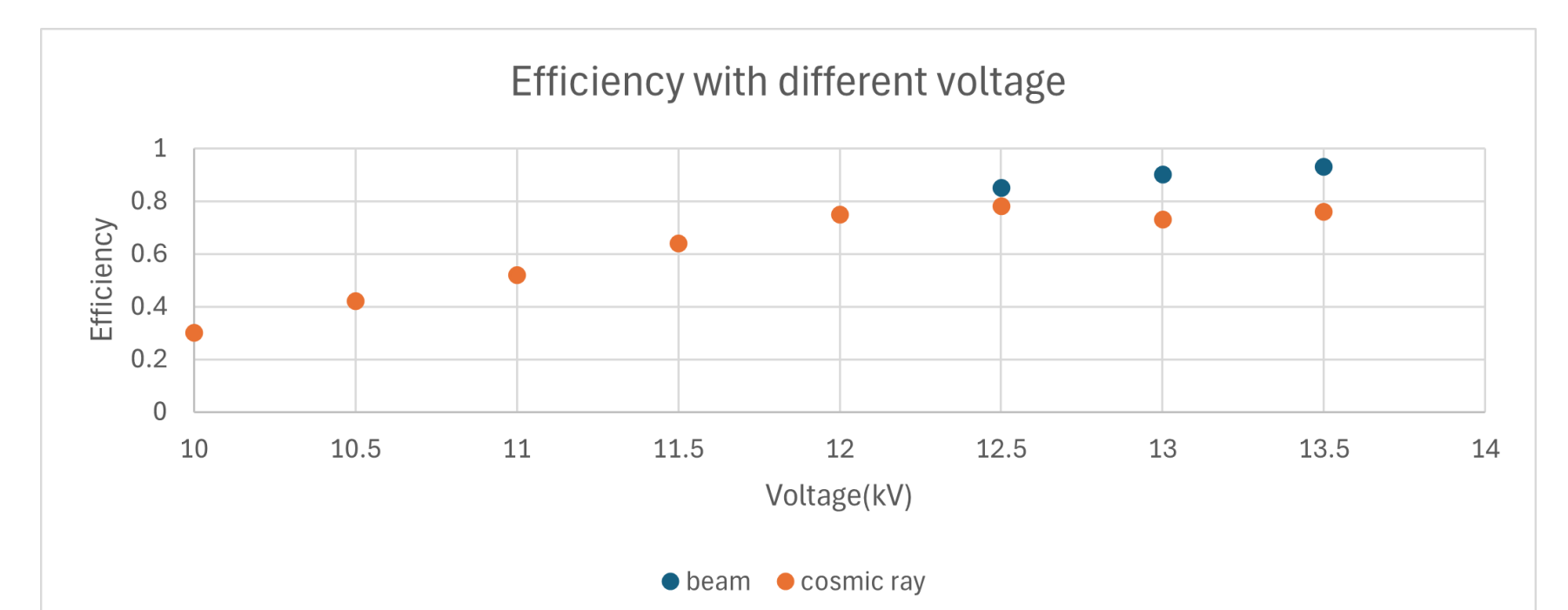


Figure 7: RPC efficiency in different voltage

We found that the efficiency of RPC using cosmic ray as source is lower than that of using electron beam as source, and this is mainly because cosmic ray is not an ideal source to test the efficiency of RPC detector for reasons below:

1. In our setup, the trigger coverage is slightly larger than the RPC detecting area, which can lead to a loss of RPC events. This discrepancy in coverage can affect the accuracy of event detection and efficiency measurements.
2. RPCs are less sensitive to low-energy particles in cosmic rays compared to scintillator counters. This difference in sensitivity can result in RPCs detecting fewer low-energy events, while scintillator counters are more effective at capturing a broader range of particle energies.

Conclusions and Outlook

In this study, we developed a DAQ system for detecting cosmic rays using a gaseous ionization RPC detector and evaluated its efficiency across different voltages. Our results confirmed that the arrival of cosmic rays, mainly muons, follows a Poisson distribution, consistent with theoretical predictions. The RPC detector's efficiency increases with voltage, saturating around 13kV applied voltage, indicating its optimal operational range using cosmic rays as source.

For future work, we plan to set up measurements to assess the timing resolution of the RPC. This will involve integrating a VMEbus system into the DAQ setup. Time-to-digital converters (TDCs) offer higher time resolution, achieving 25 picoseconds, which is significantly better than the oscilloscope we currently have, which has a resolution of 400 picoseconds. VME TDCs are optimized for managing high event rates and large data volumes, whereas oscilloscopes are better suited for real-time waveform observation rather than extensive data processing. The flow diagram of the future setup is shown below:

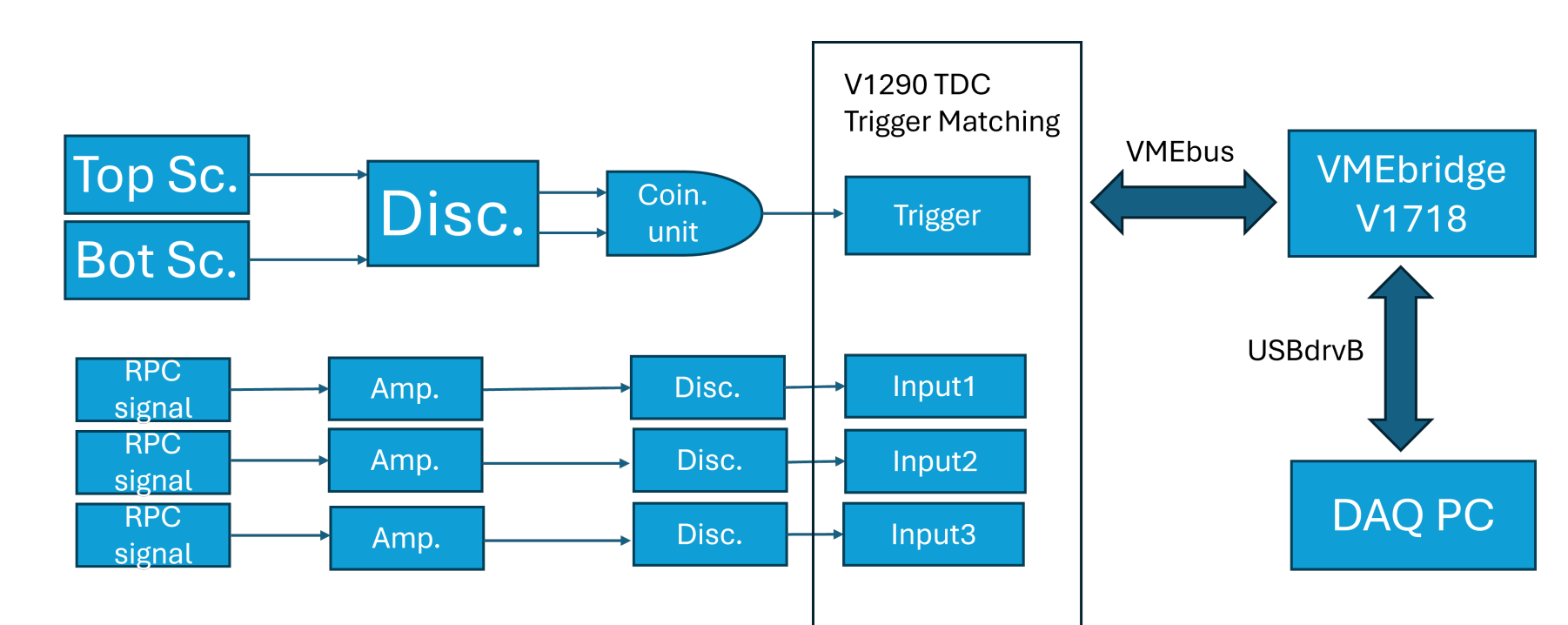


Figure 8: DAQ using VMEbus

¹M. E. Peskin and D. V. Schroeder. *An Introduction to Quantum Field Theory*. Addison-Wesley, 1995.

²W. R. Leo. *Techniques for Nuclear and Particle Physics Experiments: A How to Approach*. 1987.

³ $1/(\text{cm}^2/\text{min}) \times 3 \times 2(\text{cm}^2) = 6/(\text{min})$

